

# Silylated MCM-41 Synthesized from Rice Husk

N. Ketcome

N. Grisdanurak

*Department of Chemical Engineering*

*Faculty of Engineering*

*Thammasat University*

*Pathumtani 12120 THAILAND*

*Email: gnurak@enr.tu.ac.th*

Mesoporous material, MCM-41, synthesized from rice husk (RH-MCM-41) was modified by loading silylating agent (either Trimethylchlorosilane (TMCS), Dimethyl-dichlorosilane (DMCS) or Phenyl-trichlorosilane (PTCS)) in different concentration (1-9 %wt), and aging time, varied from 1, 6, 9 and 24 hr. Properties of samples were characterized by XRD,  $N_2$  adsorption, FTIR, and TPD and adsorption of water, hexane, and toluene. Chemical modification resulted smaller pore size average and less surface area of RH-MCM-41, from 2.9 to 2.2 nm and from 900 to 500  $m^2/g$ , respectively. PTCS could affect RH-MCM-41 surface structure more than other two. Adsorption behavior of modified RH-MCM-41 was also reflected to comparatively higher hydrophobicity.

**Keywords:** RH-MCM-41, CVOCs adsorption, and hydrophobicity.

## INTRODUCTION

Mesoporous molecular sieves, MCM-41, has utilized in many applications such as catalysis, adsorption, separation, environmental pollution control, and intrazeolite fabricating technology. The most advantageous features of these novel materials, such as large BET surface area and pore volume, hydrophobic surface nature, etc., indicate itself as a selective adsorbent. Since silica plays a key role in MCM-41 characters, the utilization of rice husk waste, which has high silica content, becomes a more interesting concept. Rice husk contains more than 20% by weight of hydrated amorphous silica. Furthermore, the process of silica extraction is very simple and inexpensive; making it beneficial to use rice husk

as a natural source of silica, instead of commercial silica. Previous work, Grisdanurak and co-workers [2003] synthesized RH-MCM-41 using sodium silicate prepared from rice husk as silica source and hexadecyltrimethylammonium bromide (CTAB) as a template. The molar composition was reported as  $1.0SiO_2: 1.1NaOH: 0.13CTAB: 121.98H_2O$ . The mesoporous structure was completely crystallized within 48 h aging at pH value of 10 and designated as RH-MCM-41. The material presented high surface area around 750-1,100  $m^2/g$  with a uniform pore size distribution and well organized in physical structure of hexagonal arrangement. Applied to CVOCs adsorption, RH-MCM-41 showed the adsorption higher than commercial mordenite and activated carbons. However, it was found

that the adsorption of chlorinated volatile organic compounds (CVOCs) is still in competition between CVOCs and water itself. To enhance the property of CVOCs adsorption capability, RH-MCM-41 is needed to be modified for being more hydrophobic.

It has been proven that material could be enhanced properties of hydrothermal stability and hydrophobicity by the silylation with silane chemicals. Up to date, this modification has been extended to other material preparations such as hydrophobic membrane [Park 2003, Yoshida 2003, Assogna 1992], adsorbent [Liu 2004, Takei 1997], and polymer-natural fiber [Imai 1998, Zakaria 2001, Ratanawong 2005]. In the case of M41S, the surface properties of mesoporous molecular sieves were changed by covalently bonding organic groups to the inorganic siliceous framework. The two strategies most commonly used to incorporate organic groups are post-synthetic silylation of the surface silanols or co-condensation of organosiloxanes with the framework silica source during hydrothermal synthesis. The chief benefits of post-synthetic silylation are simplicity and versatility, given the wide variety of commercially available silylation agents.  $\text{RSi}(\text{OEt})_3$  and  $\text{RSiCl}_3$  are the most commonly use as silylating agents. Silylated materials posses lower BET surface areas and pore volume [Capel-Sanchez 2004]. Eventhough many works have been done in the silylation to MCM-41, there is no report confirming on any surface properties of the silylation of M41S from rice husk silica. In this present work, it is a continuous work on surface modification of RH-MCM-41 in order to improve its hydrophobicity. The influence of several parameters such as the type and concentration of silylating agents, and reaction time were investigated.  $\text{N}_2$  adsorption, XRD, FTIR, and TPD were employed to analyze sample materials.

## EXPERIMENTAL PROCEDURES

### *RH-MCM-41 synthesis*

Rice husk silica was extracted from rice husk using concentrated HBr for 1 hr. After rinsed, it was burnt at 650°C for 4 h. Then it was reacted with NaOH to produce sodium silicate solution. RH-MCM-41 was prepared using sodium silicate

and hexadecyltrimethyl-ammonium bromide (CTAB) as a template. Gel composition and procedure were described previously [Grisdanurak 2003]. After aging, the suspended solid was filtered and washed with ethanol before calcined at 550°C for 6 hr under airflow.

### *Silylation procedure*

RH-MCM-41 was outgassed 4 hr at 400 mbar and 200°C, and then it was suspended in toluene under agitation, added with silylating agent (either Trimethylchlorosilane (TMCS), Dimethyl-dichlorosilane (DMCS) or Phenyl-trichlorosilane (PTCS)), refluxed at 25°C after aging then washed with toluene and dry at 100°C for 1 hr. Parameters of concentration (1–9 %wt), and aging time, varied from 1, 6, 9 and 24 hr were investigated. Samples were named according to silylating agent-concentration in %wt-aging time in hr. For example, T1-24 was designated RH-MCM-41 which was silylated by 1%TMCS within 24 hr.

### *Characterizations*

The physical structure and properties of samples were examined by spectroscopic and microscopic techniques. The study of crystallinity change was identified by XRD diffractometer, Model Bruker axS D5005 using Cu K $\alpha$  radiation. The x-ray was generated with a current of 40 mA and a potential of 40 kV. The samples were scanned from 1 to 10 degrees (2 $\theta$ ) in step of 0.5 degree per minute. Physical characteristics of the sample were determined by  $\text{N}_2$  adsorption-desorption isotherm at 77 K for relative pressure from  $10^{-2}$  to 0.99 on an AUTOSORB-1 analyzer. Before measurement, sample was degassed with heat at 250°C for 3 hr. The BET surface area was obtained from the  $\text{N}_2$  adsorption data in the relative pressure range of 0.02 to 0.2. The pore size and pore volumes were calculated from the desorption branches if the isotherm using Barrett-Joyner-Halenda (BJH) method. FTIR spectroscopy, provided the descriptions of functional groups, was carried out under 2.5 mg of sample in 90 mg KBr. The sample was scanned in range of 400-4000  $\text{cm}^{-1}$  using FTIR Spectrometer EQUINOX 55, Bruker Model.

Moisture content in parent and modified RH-MCM-41 were carried out using TPD technique. Hexane and Toluene adsorptions and TPD data were obtained from a homemade adsorption-TPD set. A certain amount of adsorbent was packed in a stainless steel tube which was connected to the gas chromatography with an FID detector and  $N_2$  as the carrier gas. Before dosing, adsorbent was heated to  $500^\circ\text{C}$  in the flow of nitrogen for 1 hr. Amount of adsorbate (hexane and toluene) was dosed by a temperature controllable saturator. Afterwards, the adsorbent was saturated with the vapor hydrocarbons under a particular temperature of  $70^\circ\text{C}$ . The desorption profile was done by increasing the temperature from 30 to  $500^\circ\text{C}$ , with a ramping rate of  $5^\circ\text{C}/\text{min}$ . For the adsorption isotherm, adsorbate was introduced within the range of relative pressure up to 0.5 using a temperature controllable saturator.

## RESULTS AND DISCUSSIONS

Parent RH-MCM-41 synthesis was investigated at different aging temperature at 48 hr. It was carried out at atmospheric pressure. XRD patterns at  $35^\circ\text{C}$ ,  $60^\circ\text{C}$ , and  $80^\circ\text{C}$  are presented in Figure 1. The patterns show Bragg peaks at low reflection angles as similar to MCM-41 XRD pattern [Kresge 1992]. There are 4 important

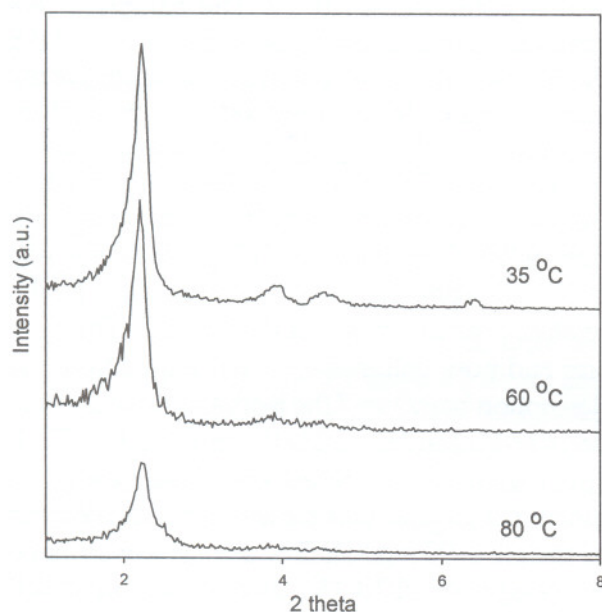


Figure 1. XRD Patterns of RH-MCM-41 at Various Temperatures and at an Aging Time of

peaks showing up in the range of 2 between 2–8 at 2.4, 4.0, 4.8, and 6.3. The reflections are due to the ordered hexagonal array of parallel silica tube and can be indexed assuming a diffraction unit cell as  $(d100)$ ,  $(d110)$ ,  $(d200)$ ,  $(d210)$ . It was observed the decrease of intensity over  $80^\circ\text{C}$ . Since the reaction was not carried out under a hydrothermal condition, it might cause the TEOS:CTABr ratio moved out from the self assembled structure boundary during the synthesis at this high temperature [Firouzi 1995]. For preventing that problem, synthesis at  $35^\circ\text{C}$  was preferred for the further study. XRD patterns of seven samples were presented in Figure 2. Modified RH-MCM-41 still show the XRD main peaks similar to the parent one, which indicates the texture of initial material remained to some extent. As observed, the main reflection peak ( $2\theta \sim 2.4$ ) intensity was decreased with the addition of functional ligand. The absence or weakness of 110, and 200 reflections was also found indicating that some diffusion and any structural order of the material did not extend over a long range. It could be usually observed during modification of mesoporous materials.

Modified RH-MCM-41 with different silylating agents, concentrations, and aging times showed insignificantly affect to material morphology in this study range.

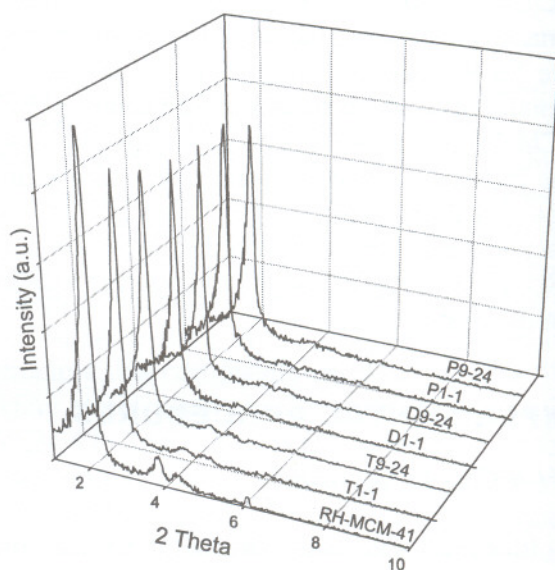


Figure 2. XRD Patterns of RH MCM-41 and Silylated RH-MCM-41

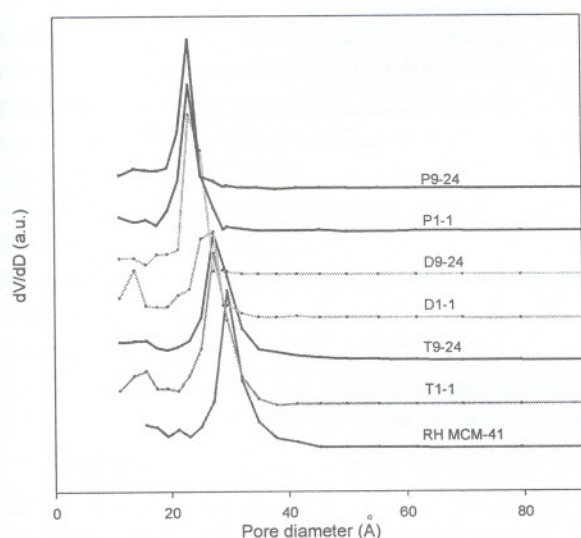


Figure 3.  $N_2$  Adsorption-Desorption at 77K of RH-MCM-41 and Silylated RH-MCM-41

**BET.** Figure 3 shows nitrogen adsorption/desorption isotherms of RH-MCM-41 samples, both before and after modification. All samples display one characteristic Type IV adsorption/desorption isotherm ascribed to mesoporous materials, where an abrupt inflection can be observed on the isotherm at the relative pressure between 0.20 and 0.40. This indicated that there was no damage significantly found during the silylation. It was observed that isotherm of silylated samples (TMCS, DMCS, and PTCS) shifted to the lower relative pressure and the flat steps of condensation got lower than parent RH-MCM-41. This might due to silylated chemical inserting into the channels. The higher concentration and aging time affected little to a corresponding sample with lower conditions. For example, samples of T9-24, D9-24, and P9-24 showed lower adsorption isotherm compared to samples of T1-1, D1-1, and P1-1, respectively. Moreover the hysteresis was also absence to some

samples explaining the reversible adsorption occurring over the range. The increase of adsorption volume in the low relative pressure region indicated that the narrowed pore entrances (to the micropore size) enhanced the adsorption potential near the pore mouth region.

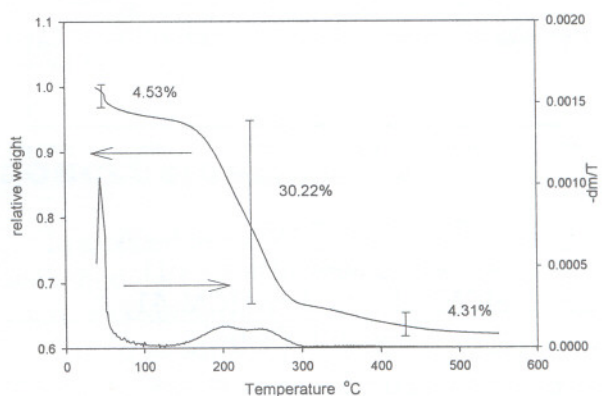


Figure 4. Pore Size Distributions of RH-MCM-41 Silylated RH-MCM-41

Figure 4 presents pore size distributions of those samples and BET surface and average pore size diameter of various samples were tabulated in Table 1. After silylation of RH-MCM-41, the BET surface area, and effective pore size had been reduced from  $\sim 900$  to  $500 \text{ m}^2/\text{g}$ , and from proximity of  $2.9 \text{ nm}$  to  $2.2 \text{ nm}$ , respectively. Micropores were also observed in the pore size distribution of some silylated RH-MCM-41, as described before. PTCS has larger molecular size compared to other. It, therefore, reduced dramatically average pore size of material more than TMCS and DMCS did.

**FTIR:** As investigated that TMCS showed little affect to its structures compared to DMCS and PTCS, we then selected a sample modified with TMCS with longer aging time, named T1-6. The sample was analyzed by FTIR in transmittance

Table 1 Textural parameters of RH MCM-41 both before and after modification.

| Sample    | BET surface area ( $\text{m}^2$ ) | Average pore size ( $\text{\AA}$ ) |
|-----------|-----------------------------------|------------------------------------|
| RH MCM 41 | 912                               | 29                                 |
| T1-1      | 721                               | 27                                 |
| T9-24     | 695                               | 27                                 |
| D1-1      | 706                               | 26                                 |
| D9-24     | 568                               | 22                                 |
| P1-1      | 608                               | 22                                 |
| P9-24     | 558                               | 22                                 |

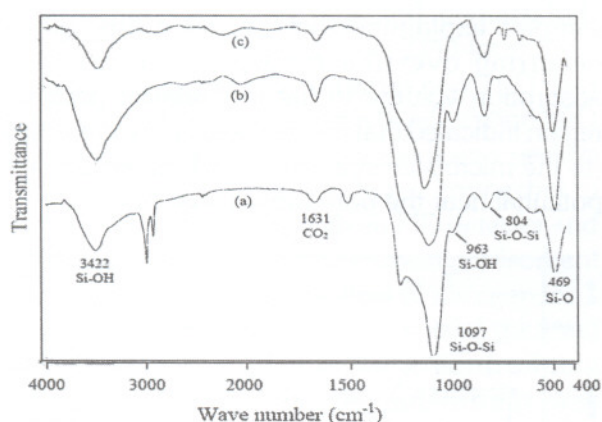


Figure 5. FTIR spectrum of (a) as-synthesized RH-MCM-41, (b) RH-MCM-41, and (c) T1-6.

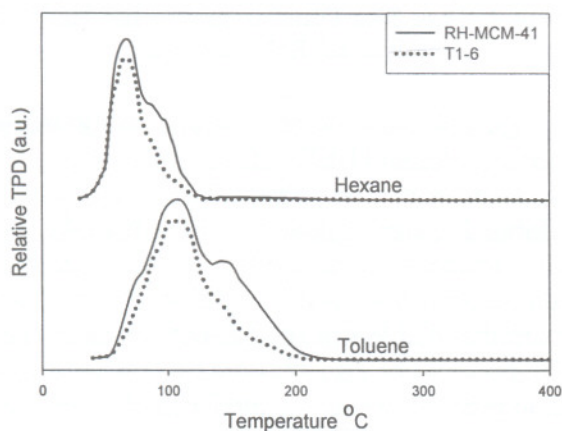


Figure 7. TPD Profiles of Hexane and Toluene on RH-MCM-41 and Silylated RH-MCM-41

modes between 4000 and 400  $\text{cm}^{-1}$  of the organic functional group RH-MCM-41 and other complexes functionalized RH-MCM-41 as shown in Figure 5. The spectrum (b) of RH-MCM-41 was similar to one described in Grisdanurak (2003). A broad transmittance band around 3422  $\text{cm}^{-1}$  was assigned to H-bonded silanols brought close to other silanols (Si-O-H) acting as proton acceptors while the peak at 963  $\text{cm}^{-1}$  was assigned to symmetric stretching vibration of Si-O-H groups. Both silanol groups were increased with calcination process because of template elimination. However, they were decreased after the silylation process by the substitution of silylate group into silanol group. Template-free RH-MCM-

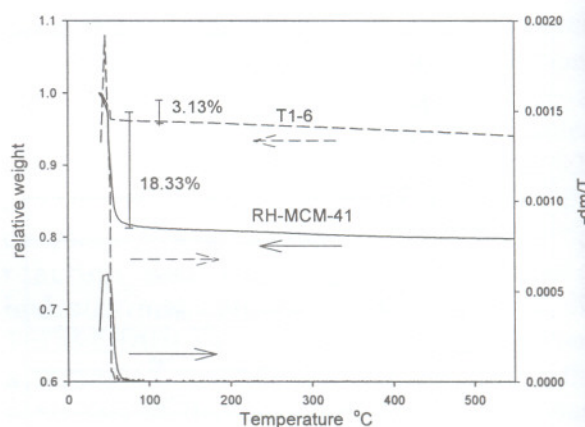


Figure 6. TPD Profiles of Vapor Water and Other Volatile Chemical from Materials (a) as Synthesized RH-MCM-41, (b) RH-MCM-41, and Silylated RH-MCM-41

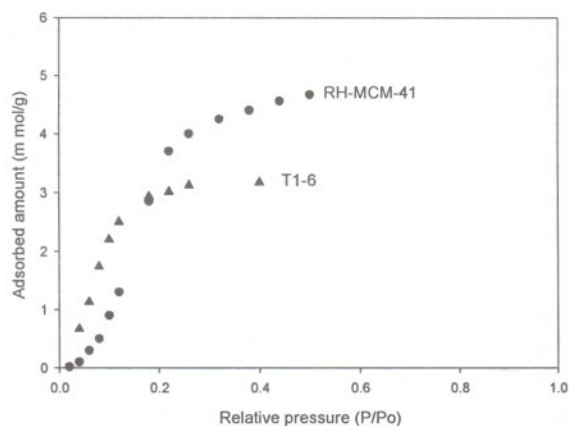


Figure 8. Toluene adsorption isotherm on RH-MCM-41 and silylated RH-MCM-41

41 showed bands at 1097 (strong), 804, and 445-469  $\text{cm}^{-1}$  as assigned to characteristic anti-symmetric stretching, vibrations of Si-O-Si bridges crosslinking the silicate network, respectively [Almeida 1990]. The spectrum after modified with O-Si((CH<sub>3</sub>)<sub>x</sub>Cl<sub>3-x</sub>) appeared Si-Cl, SiCl<sub>x</sub> peaks at around 625 (broad vibrational feature), 710 (stretching mode), 1100, 1150  $\text{cm}^{-1}$ , however, not really clear [Ferguson 2000].

TPD-water content: Applied to the adsorption application, T1-6 was further investigated to hydrophobicity test through water and non-polar chemical adsorption. Weight loss profiles and TPD spectrum of all as-synthesized RH-MCM-41, RH-MCM-41, and T1-6 obtained from TGA are

shown in Figure 6. The weight loss profiles were additionally computed in term of differential mass proportional to temperature obtained for TPD spectrum. Figure 6 (a) shows the data of as-synthesized RH-MCM-41. It was found four main peaks. Their maximum positions were located at 60, 200, 260, and 380°C. The first peak, ranged from 40-100°C with centered at 60°C, is associated with physically adsorbed water. It seemed that water was still contained into the as-synthesized after heating 105°C approximately 4.53%. The second and third peaks were quite overlapped, started from 140 to 300°C with two maxima. It should be due to the hydrocarbon template vaporization and the combustion of remaining carbon species. This corresponded to 30.22% weight loss. The last peak approximately 4.31% should be assigned for Si-OH group elimination. The remaining material was balanced to be 40%, referred to ash. RH-MCM-41 and T1-6 were examined for its moisture content, and their TPD profiles are shown in Figure 6 (b). A single straight peak of each sample was observed in the range of low temperature up to 100°C, referring to the dehydration from the sample. Approximately 18.3 and 3.13 % of water were observed, presented better hydrophobicity after the silylation.

TPD-hexane-toluene: Figure 7 shows TPD spectrum for toluene and hexane on RH-MCM-41 and T1-6. RH-MCM-41 exhibited one strong peak and a shoulder peak, while T1-6 showed one single asymmetric peak with small hump at the end. The maximum peak for each chemical desorption profile was right around each own boiling point, 68-70°C for hexane and 110°C for toluene. The observed two peaks in the TPD on RH-MCM-41 indicated the presence of two energetically different types of hexane or toluene adsorption sites (isolated Si-OH, and another Si-OH group involving H-bonds) [Jentys 1996]. The asymmetric shape of the TPD curves found on T1-6 was explained that the desorption of particular hydrocarbons was of first order, resulted from Si-OH sites were substituted by Si-((CH<sub>3</sub>)<sub>x</sub>Cl<sub>3-x</sub>) as explained by FTIR. Moreover, TPD profiles of silylated material (T1-6) were below those of RH-MCM-41. It referred that less adsorption taking place on silylated material (T1-6) compared to RH-MCM-41.

Figure 8 confirms that toluene could be absorbed onto T1-6 less than RH-MCM-41. It might due to less surface area presenting after the silylation, however, adsorption behaviors were different from each other. RH-MCM-41 still shows a type IV adsorption, while T1-6 behaves closely to Langmuir isotherm. The difference indicates that silylation can enhance the oleophilic property of RH-MCM-41.

## CONCLUSIONS

In this study, the utilization of rice husk silica was introduced to MCM-41 synthesis. Moreover, it was modified by three kinds of silylating reagents to improve its surface properties. Concentration and aging time were studied parameters. Bulk structure of modified RH-MCM-41 remained unaffected with increasing concentration and aging time, while the BET surface area and average pore size were little dependent on silylating reagent. The adsorption isotherm data consistently showed typical type IV of IUPAC classifications for all studied samples. The adsorption of water vapor was dramatically decreased by silylation, indicating that hydrophobicity was enhanced.

## ACKNOWLEDGMENT

Authors are grateful to The National Research Council of Thailand (NRCT 2004-2005) and The Shell (Thailand) Centenary Scholarship Fund (Graduate research 2005) for financial supports to this work.

## REFERENCES

- Assogna, A., Perego, G., Roggero, A., Sisto, R., and Valentini, C. (1992). "Structure and gas permeability of silylated polyphenylene oxide," *J Membrane Sci.*, 71, 97-103.
- Capel-Sanchez, M.C., Barrio, L., Campos-Martin, J.M., Fierro, J.L.G. (2004) "Silylation and surface properties of chemically grafted hydrophobic silica," *J Colloid Interf Sci.*, 277, 146-153.

- Chen, C-Y., Xiao, S-Q., and Davis, M. E. (1995). "Studies on Ordered mesoporous materials III. Comparison of MCM-41 to mesoporous materials derived from kanemite," *Micropor Mater.*, 4, 1-20.
- Firouzi, A., Kumar, D., Bull, L. M., Besier, T., Sieger, P., Huo, Q., Walker, S.A., Zasadzinski, J. A., Glinka, ., Nicol, J., Margolese, D. I., Stucky, G. D. and Chmelka, B. F. (1995). "Cooperative Organization of Inorganic-Surfactant and Biomimetic Assemblies," *Science.*, 267, 1138-1143.
- Grisdanurak, N., Chiarakorn, S., and Wittayakun, J. (2003). "Utilization of Mesoporous Molecular Sieves Synthesized from Natural Source Rice Husk Silica to Chlorinated Volatile Organic Compounds (CVOCs) Adsorption," *Korean J Chem Eng.*, 20 (5), 950-955.
- Imai, Y., and Oishi, Y. (1989). "Novel synthetic methods for condensation polymers using silylated nucleophilic monomers," *REV Prog Polym Sci.*, 14, 173-193.
- Jentys, O.A., Pham, N.H., Vinek, H., Englisch, M., and Lercher, J.A. (1996). "Synthesis and characterization of mesoporic materials containing highly dispersed cobalt" *Micropor Mater.*, 6, 13-17.
- Liu, C., Naismith, N., and Economy, J. (2004). "Advanced mesoporous organosilica material containing microporous  $\beta$ -cyclodextrins for the removal of humic acid from water." *J Chromatogr A.*, 1036, 113-118.
- Maria Chong, A. S., Zhaoa, X. S., Kustedjo, T., and Qiao, S.Z., (2004). "Functionalization of large-pore mesoporous silicas with organosilanes by direct synthesis," *Micropor Mesopor Mat.*, 72, 33-42.
- Nishiyama, N., Park, D-H., Egashira, Y., and Ueyama, K. (2003). "Pore size distributions of silylated mesoporous silica MCM-48 membranes," *Separ Purif Technol.*, 32, 127-132.
- Park, D-H., Nishiyama, N., Egashira, Y., and Ueyama, K. (2003). "Separation of organic/water mixtures with silylated MCM-48 silica membranes" *Micropor Mesopor Mat.*, 66, 69-76.
- Ratanawong, O., Grisdanurak, N., Kaewsrichan, L. (2005). "Adsorption of oil emulsified in water with modified oil palm fruit fiber," *P. S. J Sci Tech.*, XX, XX-XX (*In press, Thai*).
- Selvan, P., Bhatia, S. K., and Sonwane, C. G. (2001). "Recent Advances in Processing and Characterization of Periodic Mesoporous MCM-41 Silicate Molecular Sieves," *Ind Eng Chem Res.*, 40, 3237-3261.
- Takei, T., Yamazaki, A., Watanabe, T., and Chikazawa, M. (1997). "Water Adsorption Properties on Porous Silica Glass Surface Modified by Trimethylsilyl Groups," *J Colloid Interf Sci.*, 188, 409-414.
- Yoshida, W., and Cohen, Y. (2003). "Topological AFM characterization of graft polymerized silica membranes," *J Membrane Sci.*, 215, 249-264.
- Zakaria, S., Hamzah, H., Murshidi, A. J., and Deramen, M. (2001). "Chemical Modification on Lignocellulosic polymeric oil palm empty fruit bunch for advanced material," *Adv Polym Tech.*, 20 (4), 289-295.
- Zheng, S., Gao, L., and Guo, J. (2001). "Synthesis and characterization of copper(II)-phenanthroline complex grafted organic groups modified MCM-41," *Mater Chem Phys.*, 71, 174-178.